Chaotic Modeling and Simulation (CMSIM) 2: 133–146, 2020

Prediction of Horseshoe Chaos in a Nonlinearly Damped Asymmetrical Systems

S. Valli Priyatharsini[1], B. Bhuvaneswari[1], V. Chinnathambi[1] and S. Rajasekar[2]

[1] Department of Physics, Sadakathullah Appa College, Tirunelveli-627 011, Tamil Nadu, India.(Affiliated to Manonmaniam Sundaranar University, Tirunelveli-627012, Tamil Nadu, India)
(E-mail: drchinnathambi@sadakath.ac.in)

[2] School of Physics, Bharathidasan University, Tiruchirapalli-620 024, Tamil Nadu, India.
(E-mail: rajasekar@cnld.bdu.ac.in)

Abstract. The occurrence of horseshoe chaos in a nonlinearly damped Duffing-vander Pol (DVP) oscillator with three different forms of asymmetrical double-well potential is analyzed. Three forms of asymmetry can be introduced by varying the depth of the left-well alone, the location of the local minimum of the left-well alone and both the depth and local minimum of the left-well respectively, keeping the shape of the right-well unchanged. We assume the nonlinear damping term is proportional to the power of velocity ($\dot{x}$) in the form $|\dot{x}|^{P-1}$. Applying the Melnikov analytical technique, the threshold condition for the occurrence of horseshoe chaos is obtained for each asymmetrical potential. Melnikov threshold curves are drawn in $(f-\omega)$ parameter space. By varying the parameter f, parametric regimes where suppression or induce of chaos are predicted. The analytical predictions are verified by numerical simulation.

1 Introduction

Over the past years the possibility of horseshoe dynamics for periodically forced symmetric and asymmetrical systems with linear damping has become a well established fact [1–10]. In recent years there has been a great deal of interest on the study of nonlinearly damped nonlinear systems [11–25]. In the present work we wish to study the occurrence of horseshoe chaos in a nonlinearly damped Duffing-vander Pol oscillator with three different asymmetric double-well potentials both analytical and numerical techniques.

A horseshoe is the occurrence of a transverse intersection of the stable and unstable manifolds of a saddle fixed point in the Poincaré map and is a global phenomenon [1,2]. The appearance can be predicted analytically by employing the Melnikov technique [1,2,26–32]. This technique essentially gives

Received: 15 January 2020 / Accepted: 25 April 2020

ISSN 2241-0503

a criterion for a transverse intersection of the stable and unstable manifolds of the homoclinic / heteroclinic orbits which imply *horseshoe chaos*.

The equation of motion of a nonlinearly damped Duffing-vander Pol (DVP) oscillator is given by

$$\ddot{x} + \gamma\ \dot{x}\ (1 - x^2)\ |\dot{x}|^{p-1} + \frac{dV_i}{dx} = f \sin \omega t, \tag{1}$$

where x stands for the displacement from the equilibrium position, p is the damping exponent, $\gamma > 0$ is the damping parameter of the system and f and ω are the amplitude and frequency of the external time dependent periodic driving force. We consider three different asymmetric double-well potentials V_1, V_2 and V_3 is given by

$$V_i(x) = \begin{cases} -\frac{1}{2}\omega_0^2 x^2 + \frac{1}{4}\beta x^4, & x \geq 0 \\ -\frac{1}{2}A_i\omega_0^2 x^2 + \frac{1}{4}B_i\beta x^4, & x < 0 \end{cases} \tag{2}$$

where $i = 1, 2, 3$, $A_1 = B_1 = \alpha$, $A_2 = 1/\alpha^2$, $B_2 = A_2^2$, $A_3 = 1$, $B_3 = 1/\alpha^2$ and ω_0^2, α and $\beta > 0$. In V_1, V_2 and V_3 the depth of the left-well alone, the location of the local minimum of the left-well alone and both the depth and the local minimum of the left-well respectively can be varied by the control parameter α by keeping the shape of the right-well unchanged. For V_1 the unperturbed system is

$$\ddot{x} - \omega_0^2 x + \beta x^3 = 0 \qquad x \geq 0 \tag{3}$$

$$\ddot{x} - \alpha(\omega_0^2 x - \beta x^3) = 0 \qquad x < 0 \tag{4}$$

Similarly, we can write the equation of motion separately for $x \geq 0$ and $x < 0$ for the system with the potentials V_2 and V_3. We call the systems with the asymmetric potentials V_1, V_2 and V_3 as system-1, system-2 and system-3 respectively. Figure 1 depicts the effect of the asymmetry parameter α on the three potentials for $\beta = 5.0$ and $\omega_0^2 = 1.0$. A similar nonlinear damping term [15,16,20,23,24,33,34]and asymmetric potentials [8,35–37] was previously used by many researchers.

The objective of the present work is to analyze influence of the asymmetry parameter α and damping exponent P on the onset of homoclinic chaos, asymptotic cross-well chaos and bifurcation phenomenon in the DVP system with the three distinct potentials V_1, V_2 and V_3. To get an analytical expression for the onset of homoclinic chaos (horseshoe chaos) we can use the Melnikov analytical method. Using the Melnikov method we analyze the role of asymmetry parameter α on the onset of homoclinic chaos in the left-well and in the right-well. Then we carry out numerical study on the onset of asymptotic chaos and bifurcation phenomenon. We find certain interesting and nontrivial results.

To be specific, in Section 2, we present the calculation of Melnikov function for the three asymmetrical systems. In Section 3, we obtain the Melnikov threshold condition for the transverse intersections of homoclinic orbits for nonlinearly damped DVP system separately for each of the asymmetric system. We

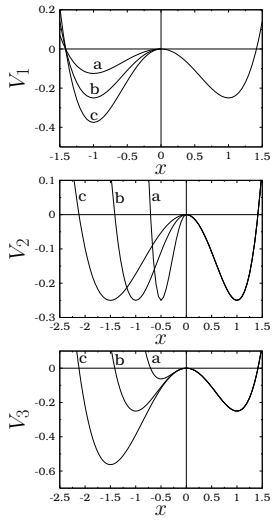

Fig. 1. The potentials V_1, V_2 and V_3 for three values of α. In all the subplots the potential curves **a**, **b** and **c** correspond to $\alpha = 0.5$, 1 and 1.5 respectively. $\alpha = 1$ corresponds to the symmetric double-well potential The other parameters are fixed as $\omega_0^2 = 1$ and $\beta = 5$.

plot the Melnikov threshold curve in $(f - \omega)$ parameter plane for all the systems where f and ω are the amplitude and frequency of the external periodic sinusoidal force. We verify the analytical prediction with the numerically calculated critical values of f at which the transverse intersections of homoclinic orbits in Section 4. Finally Section 5 contains the concluding remarks.

2 Calculation of Melnikov Functions for the Three Asymmetric Potentials

The equation of motion of the perturbed systems corresponding to the potentials V_1, V_2 and V_3 are given by

$$\dot{x} = y \tag{5}$$

$$\dot{y} = -\frac{dV_i}{dx} + \epsilon[-\gamma\ \dot{x}\ (1 - x^2)|\dot{x}|^{p-1} + f \sin \omega t] \tag{6}$$

where $i = 1, 2, 3$ and ϵ is a small parameter so that the damping and forcing terms are perturbations to the cubic oscillator. In a very recent work, Sethu Meenakshi et al. [33,34] studied the effect of amplitude modulated signal in nonlinearly damped symmetrical DVP system. The homoclinic orbits of the unperturbed system ($\epsilon = 0$) with the potentials V_1, V_2 and V_3 are given by

$$x_{i,h}(t) = \begin{cases} x_{i,h}^{+}(t) = \sqrt{\frac{2\omega_0^2}{\beta}}\ \mathrm{sech}(\sqrt{\omega_0^2}t), & x \geq 0 \\ \\ x_{i,h}^{-}(t) = -\sqrt{\frac{2\omega_0^2}{\beta}}\ \lambda_i\ \mathrm{sech}(\delta_i t) & x < 0 \end{cases} \tag{7}$$

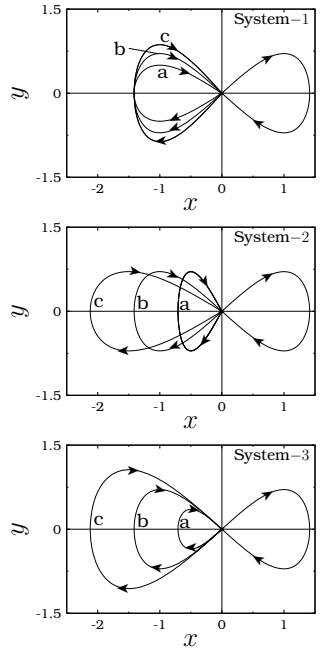

Fig. 2. Homoclinic orbits of the three unperturbed systems for $\alpha = 0.5$(a), 1 (b) and 1.5 (c). The other parameters are fixed as $\omega_0^2 = 1$ and $\beta = 5$.

and

$$y_{i,h}(t) = \begin{cases} y_{i,h}^{+}(t) = -\omega_0^2 \sqrt{\frac{2}{\beta}}\, \mathrm{sech}(\sqrt{\omega_0^2}t)\times \\ \tanh(\sqrt{\omega_0^2}t), & x \geq 0 \\ y_{i,h}^{-}(t) = q_i\ \omega_0^2 \sqrt{\frac{2}{\beta}}\, \mathrm{sech}(\delta_i\omega_0^2 t)\times \\ \tanh(\delta_i\omega_0^2 t) & x < 0 \end{cases} \tag{8}$$

where $i = 1, 2, 3$ and $\lambda_1 = q_2 = \delta_3 = 1$, $\lambda_2 = \lambda_3 = q_1 = q_3 = \delta_1 = \alpha$ and $\delta_2 = 1/\alpha$. The part of the homoclinic orbits moving away from the saddle point in the region $x < 0$ and $x > 0$ are termed as unstable manifolds W_u^- and W_u^+ respectively. Similarly the saddle W_s^- and W_s^+ are the stable manifolds approaching the saddle in the regions $x < 0$ and $x > 0$ respectively. Figure 2 shows the phase portrait of the unperturbed three asymmetrical systems for $\alpha = 0.5, 1.0$ and 1.5 with $\omega_0^2 = 1$ and $\beta = 5$.

For a system of the form

$$\dot{x} = f_1(x, y) + \epsilon g_1(x, y, t) \tag{9}$$

$$\dot{y} = f_2(x, y) + \epsilon g_2(x, y, t) \tag{10}$$

where g_1 and g_2 are periodic in t with period T. For a standard form of Eqs.(9-10), the Melnikov integral is

$$M(t_0) = \int_{-\infty}^{+\infty} h_0(X_h(\tau)) \wedge h_1(X_h(\tau), t) \times exp\left[-\int_0^T trace\left[D_X(h_0(X_h(s)))\right] ds\right] dt \tag{11}$$

where $X_h = (x_h, y_h)$ represents homoclinic orbits, $h_0 = (f_1, g_1)$, $h_1 = (f_2, g_2)$, $h_0 \wedge h_1 = f_1 g_2 - f_2 g_1$ and D_X denotes the partial derivatives with respect to X. The homoclinic orbits of the three unperturbed asymmetrical systems are different in the left-well and right-well. Therefore the analytical expression for $M(t_0)$ will be different for $x < 0$ and $x > 0$.

For the asymmetrical DVP systems Eqs.(5-6), the Melnikov function is

$$M^{\pm}(t_0) = -\gamma \int_{-\infty}^{+\infty} |y_h^{\pm}|^{P+1} dt \int_{-\infty}^{+\infty} y_h^{\pm} f \sin \omega t \, dt \tag{12}$$

where $'+'$ and $'-'$ signs refer to the regions $x > 0$ and $x < 0$ respectively. The Melnikov function $M^{\pm}(t_0$ for the three systems are calculated as

$$M_{1,2,3}^{+}(t_0) = M^{+}(t_0) = A + B + \frac{fc}{\alpha} \operatorname{sech}(D/\alpha) \times \cos \omega t_0 \tag{13}$$

$$M_1^{-}(t_0) = -A\, \alpha^P + \frac{fc}{\alpha} \operatorname{sech}(D/\alpha)\, \cos \omega t_0 \tag{14}$$

$$M_2^{-}(t_0) = -A\, \alpha + \alpha^2 fc \operatorname{sech}(D\, \alpha)\, \cos \omega t_0 \tag{15}$$

$$M_3^{-}(t_0) = -A\, \alpha^{P+1} + \alpha fc \operatorname{sech}(D)\, \cos \omega t_0. \tag{16}$$

where

$$A = -\gamma(\omega_0^2)^{p+\frac{1}{2}} \left[\frac{2}{\beta}\right]^{\frac{p+1}{2}} B\left[\frac{p+2}{2}, \frac{p+1}{2}\right] \tag{17}$$

$$B = \gamma(\omega_0^2)^{p+\frac{3}{2}} \left[\frac{2}{\beta}\right]^{\frac{p+3}{2}} B\left[\frac{p+2}{2}, \frac{p+3}{2}\right] \tag{18}$$

$$C = \sqrt{\frac{2}{\beta}}\, \pi\omega \tag{19}$$

$$D = \pi\omega/2\sqrt{\omega_0^2}. \tag{20}$$

3 Analytical results

In this section we analyze the analytical results for the occurrence of horseshoe chaos in system-1, system-2 and system-3. The intersection of the homoclinic orbits, that is intersections of stable and unstable manifolds are the necessary conditions for the existence of horseshoe chaos. Homoclinic bifurcation occurs

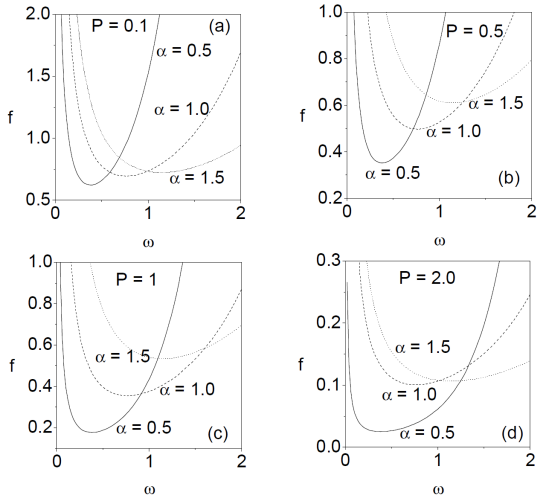

Fig. 3. Melnikov threshold curves for homoclinic intersections in $(f-\omega)$ parameter plane for fixed values of α and P for the system-1. The other parameters are fixed as $\omega_0^2 = 1.0, \gamma = 0.4$ and $\beta = 5.0$.

when $M(t_0)$ has a simple zero and changes sign. The necessary conditions on the parameters of the systems for horseshoe chaos can be obtained from the Eqs.(13-20). For all the three systems the threshold condition for horseshoe chaos in the right-well is given by

$$\mid f \mid \geq \mid f_M^+ \mid = \frac{\mid A+B \mid}{\mid C \mid} \cosh(D) \tag{21}$$

We can obtained similar conditions for horseshoe chaos in the left-well for the three systems and denote the threshold values of f as f_M^-. In general $f_M^+ \neq f_M^-$ for $\alpha \neq 1$ and $f_M^+ = f_M^-$ for $\alpha = 1$. The threshold conditions for horseshoe chaos for the system-1, system-2 and system-3 in the left-well are as follows

$$\mid f \mid \geq \mid f_M^- \mid = \frac{\mid A \mid}{\mid C \mid} \cosh(D/\alpha)\ \alpha^{P+1} \tag{22}$$

$$\mid f \mid \geq \mid f_M^- \mid = \frac{\mid A \mid}{\mid C \mid} \cosh(D\alpha)\ \alpha^{P-1} \tag{23}$$

$$\mid f \mid \geq \mid f_M^- \mid = \frac{\mid A \mid}{\mid C \mid} \cosh(D)\ \alpha^{P} \tag{24}$$

Threshold curves for horseshoe chaos can be from the Eqs.(21-24) in (f, ω) parameters space. We fix the parameters values as $\beta = 5.0, \gamma = 0.4, P = 0.1, 0.5, 1.0, 2.0$ and $\alpha = 0.5, 1.0, 1.5$. A typical plot of $f_M^{\pm}$ against ω is shown in Figure 3 for the system-1 with the fixed values of α and P. Below the threshold

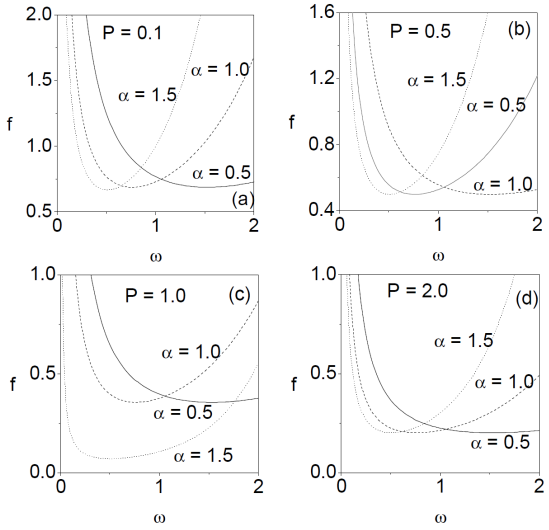

Fig. 4. Melnikov threshold curves for homoclinic intersections in $(f-\omega)$ parameter plane for fixed values of α and P for the system-2. The other parameters are fixed as $\omega_0^2 = 1.0, \gamma = 0.4$ and $\beta = 5.0$.

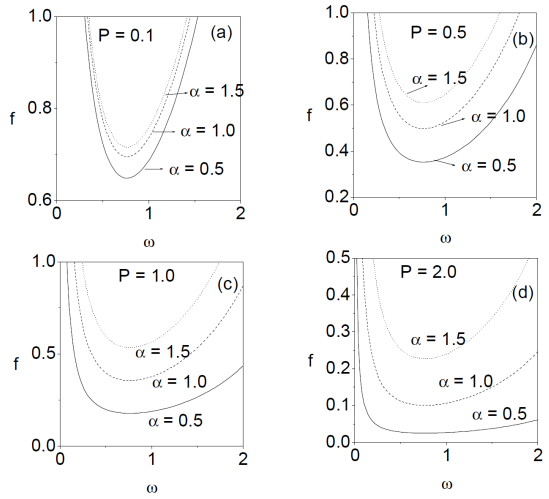

Fig. 5. Melnikov threshold curves for homoclinic intersections in $(f-\omega)$ parameter plane for fixed values of α and P for the system-3. The other parameters are fixed as $\omega_0^2 = 1.0, \gamma = 0.4$ and $\beta = 5.0$.

curves, no transverse intersection of stable and unstable manifolds of the saddle occurs and above the threshold curve, the transverse intersection of orbits of the saddle occurs. Threshold curves for onset of horseshoe chaos in the (f, ω) parameters plane for the system-2 and system-3 are plotted in Figure 4 and

Figure 5. As a result our analytical investigations using Melnikov method, we have found certain interesting and nontrivial results.

- Threshold curves are nonlinear for all the systems.
- Threshold curves are nonintersecting and smooth variation of f_M is found only in the system-3 but in system-1 and system-2 the threshold curves are intersecting with each other.
- One clear observation from the Figure 5 is that for $\alpha < 1$ the occurrence of the right-well homoclinic bifurcation alone cannot be observed for any set of values of (f, ω). Similarly $\alpha > 1$ the left-well homoclinic intersection alone is not possible.
- In system-1 and system-2, for a particular values of ω the threshold values $f_M^- = f_M^+$. For example, in Figure 3(a) for $P = 0.1$, $f_M^- = f_M^+ = 0.75$ at $\omega = 1.0$ with $\alpha = 1.0$ and 1.5. For $\omega = 0.52$, $f_M^- = f_M^+ = 0.72$ with $\alpha = 0.5$ and 1.0. Similarly in system-2, the threshold curves for $\alpha = 0.5$ and 1.0 meet at $\omega = 1.02$ and for $\alpha = 1.0$ and 1.5 meet at $\omega = 0.65$ which are clearly shown in Figure 4(a).
- In system-3 for each value of α ($\alpha \neq 1$) and P, f_M^- is always different from f_M^+ that is $f_M^- \neq f_M^+$. For example, in Figure 5(a) for $P = 0.1, \omega = 1.0$, $f_M^- = 0.65$ for $\alpha = 0.5$ and $f_M^+ = 0.72$ for $\alpha = 1.0$. Similar dynamics is observed for all values of P and α.
- In system-3 when P increases from small values the threshold values $f_M^{\pm}$ decreases, which is clearly evident in Figure 5.

4 Numerical results

In the previous section we focussed our study on analytical prediction of threshold values of control parameter f for transverse intersections of homoclinic orbits. In this section we numerically integrate the equation of motion of the three asymmetrical systems and verify the analytical results obtained from the Melnikov analytical technique. First we consider the system-1. For $\alpha = 0.5, P = 0.5$ and $\omega = 1.0$, we find $f_M^- = 0.8616$ and $f_M^+ = 0.5275$, that is system-1 has $f_M^- > f_M^+$. In this case, when f is varied from a small value, we have the scenario of no transverse intersection of stable and unstable parts of W^+ and W^- for $0 < f < f_M^+$; transverse intersection of the manifolds W_s^+ and W_u^- in the right-well alone for $f_M^+ < f < f_M^-$ and intersection of the stable and unstable parts of W^+ and W^- in the two-wells for $f > f_M^-$. Figure 6 shows numerically computed stable and unstable manifolds of homoclinic orbits for three values of f. No intersection of stable and unstable parts of W^+ and W^- occur for $f < f_M^+$ (Figure 6(a)). In Figure 6(b) where $f = 0.65$ lying between f_M^+ and f_M^- intersection of the stable and unstable parts of W^+ alone are seen. For $f = 0.9$ that is $f > f_M^-$, intersections both the left-well and right-well orbits occur (Figure 6(c)).

For system-2 with $\alpha = 0.5, P = 0.5$ and $\omega = 0.5$ we find $f_M^- = 0.3865$ and $f_M^+ = 0.5995$, that is the system-2 has $f_M^- < f_M^+$. In this case, when f is varied from a small value, transverse intersection of manifolds of the saddle in the right-well is not possible but other cases are possible. For $f < f_M^-$

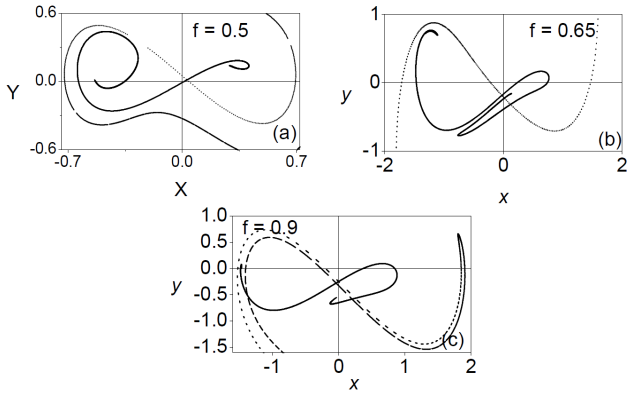

Fig. 6. Numerically computed stable and unstable manifolds of saddle for three values of f for the system-1. The values of the other parameters are $\gamma = 0.4$, $\alpha = 0.5$, $\beta = 5.0$, $\omega_0^2 = 1.0$, $\omega = 1.0$ and $P = 0.5$.

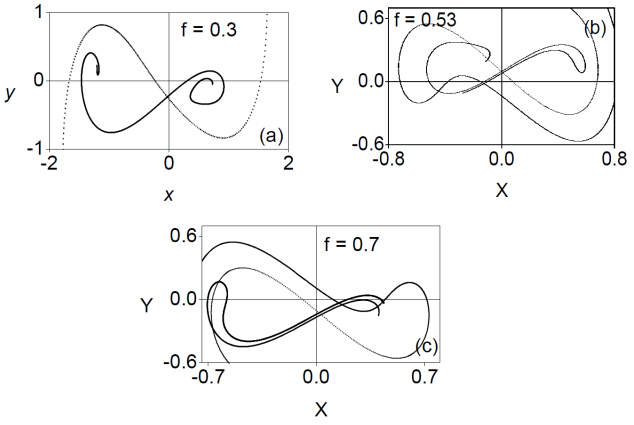

Fig. 7. Numerically computed stable and unstable manifolds of saddle for three values of f for the system-2. The values of the other parameters are $\gamma = 0.4$, $\alpha = 0.5$, $\beta = 5.0$, $\omega_0^2 = 1.0$, $\omega = 1.0$ and $P = 0.5$.

transverse intersection of the stable and unstable manifolds W^+ and W^- occur (Figure 7(a)). In the interval $0.3865 < f < 0.5995$, homoclinic intersections of W^+ and W^- alone occur in the left-well (Figure 7(b)) and transverse intersections of both the left-well and right-well orbits occur for $f > 0.5995 (= f_M^+)$ (Figure 7(c)). Similar dynamics is found in system-3 also. For example when $\alpha = 0.5, P = 0.5$ and $\omega = 1.0$, Melnikov threshold values are $f_M^- = 0.373$ and $f_M^+ = 0.5275$. As shown in Figure 8(a) for $f = 0.32 < f_M^-$, no transverse intersections occur; at $f = 0.45$ (Figure 8(b)) which lies between (f_M^-, f_M^+) transverse intersections of the left-well manifolds alone occur and for $f = 0.65 > f_M^+$ (Figure 8(c)) the stable and unstable parts of W^+ and W^- of both wells inter-

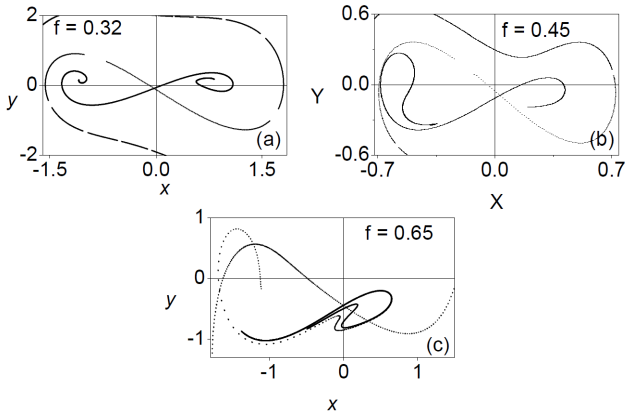

Fig. 8. Numerically computed stable and unstable manifolds of saddle for three values of f for the system-3. The values of the other parameters are $\gamma = 0.4$, $\alpha = 0.5$, $\beta = 5.0$, $\omega_0^2 = 1.0$, $\omega = 1.0$ and $P = 0.5$.

sect. Above the threshold curves it is possible to have either asymptotic chaos

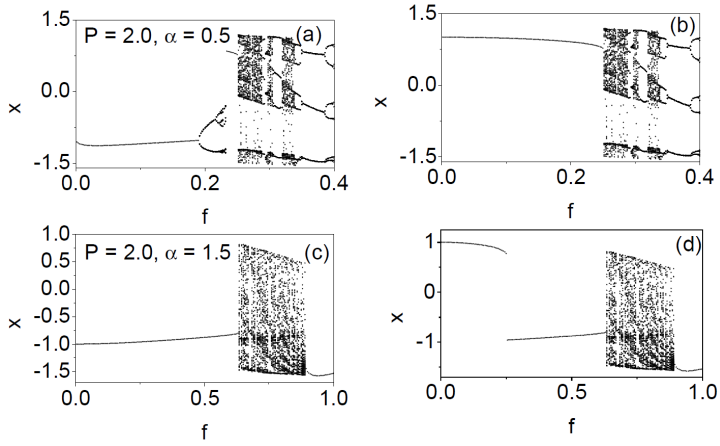

Fig. 9. Bifurcation diagrams of the system-1 with (a) the initial condition chosen in the left-well and (b) the initial condition chosen in the right-well for the starting value of f for $\alpha = 0.5, 1.5$, $\omega = 0.5, \gamma = 0.4$ and $P = 2.0$.

or transient chaos followed by asymptotically periodic motion. In order to know the nature of attractors of the nonlinearly damped system near the horseshoe threshold curve we have further numerically studied the Eq.(1) and the onset of cross-well chaos. Figure 9(a) and Figure 9(b) show two bifurcation diagrams of the system-1, one with the initial conditions chosen in the left-well and other with the initial conditions chosen in the right-well for the starting value of f.

The value of the other parameters are $P = 2.0, \alpha = 0.5, \omega_0^2 = 1, \beta = 5$ and $\omega = 1.0$. In the left-well (Figure 9(a)) at $f = 0.2316$ (which is close to the Melnikov threshold value $f_M^- = 0.2245$), the periodic orbits become unstable and the trajectories with various initial conditions jump to the right-well after a long transient and remains there forever. When the initial conditions chosen in the right-well, the bifurcation pattern is completely different, only period-T orbit occurs in the interval $0 < f < 0.2316$. At f = 0.2316 onset of cross-well chaos occurs and at which the chaotic attractor jumps from right-well to left-well. In Figure 9(c) and Figure 9(d) we analyze the case for $\alpha > 1$ ($\alpha = 1.5$) with the initial conditions chosen in the left- and right-wells for the starting value of f. Transcritical bifurcation occurs in Figure 9(d) but it is absent in Figure 9(c). Similar dynamics can be observed in system-2 and system-3 also near the horseshoe threshold.

Figure 10(a) and Figure 10(b) show the bifurcation diagrams of linearly damped ($P = 1$) asymmetrical system-1 for $\alpha = 0.5$ and $\alpha = 1.5$ with the initial condition chosen in the right-well. Figure 11 shows the bifurcation diagrams of of linearly damped ($P = 1$) system-1 for $f \in [0.0, 0.15]$ and $\alpha = 0.9$ with the initial conditions chosen in the left-well (Figure 11(a)) and in the right-well (Figure 11(b)). Suppression or enhancement of chaos is observed in both wells due to the nonlinear damping (P) term, which is clearly evident in Figures 9, Figure 10 and Figure 11.

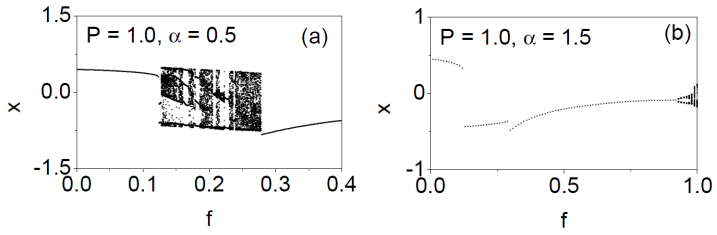

Fig. 10. Bifurcation diagrams of the system-1 with the initial condition chosen in the right-well for the starting value of f for $\alpha = 0.5, 1.5$, $\omega = 1.0, \gamma = 0.4$ and $P = 1.0$.

5 Conclusion

In this paper we considered a nonlinearly damped and periodically driven Duffing-vander Pol oscillator with three asymmetric potentials. We investigated the occurrence of horseshoe chaos by varying the control parameter f both analytical and numerical techniques. Applying Melnikov analytical technique we obtained the threshold condition for onset of horseshoe chaos. Threshold curves are drawn on (f, ω) parameters space which is separate the chaotic and periodic motions. For nonlinearly damped ($P \neq 1$) asymmetrical system-3, our study shows that Melnikov threshold values ($f_M^{\pm}$) decrease when the damping exponent increases. In the asymmetrical system-1 and system-2, for a par-

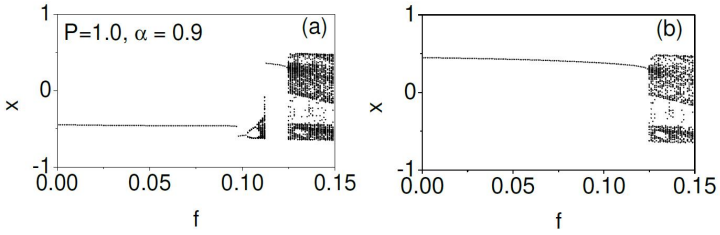

Fig. 11. Bifurcation diagrams of the system-1 with (a) the initial condition chosen in the left-well and (b) the initial condition chosen in the right-well for the starting value of f for $\alpha = 0.9$, $\omega = 1.0, \gamma = 0.4$ and $P = 1.0$.

ticular values of ω the the threshold values $f_M^- = f_M^+$ like symmetrical ($P = 1$) DVP system. For a certain range of values of the control parameter f there is a possibility to suppress and enhancement of chaos in the left- and right-wells. Furthermore it would be important to analyze the occurrence of various nonlinear phenomena such as hysteresis, coexistence of multiple attractors, stochastic resonance, vibrational resonance and Ghost-vibrational resonance

References

1. J. Guckenheimar and P. Holmes, *The Nonlinear Oscillations, Dynamical Systems and Bifurcations of Vector Fields*, Springer, New York, 1983.
2. S. Wiggins, *Introduction to Applied Nonlinear Dynamical Systems and Chaos*, Springer, New York, 1990.
3. W. Szemplinska-Stupnicka, The analytical predictive criteria for chaos and escape in nonlinear oscillators: A survey, *Nonlinear Dynamics*, vol.7: 129-147, 1995.
4. F.C Moon and G.X. Li, Fractal Basin Boundaries and Homoclinic Orbits for Periodic Motion in a Two-Well Potential, *Phys. Rev. Lett.*, vol.55: 1439-1442, 1985.
5. M. Siewe Siewe, F.M. Moukam Kakmeni and C. Tchawona, Resonant Oscillation and Homoclinic Bifurcation in a ϕ^6-Vander Pol Oscillator, *Chaos, Solitons and Fractals*, vol.21: 841-853 2004.
6. L. Ravisankar, V. Ravichandran and V. Chinnathambi, Predictions of Horseshoe chaos in DVP oscillator driven by different periodic forces, *Int. J. of Eng. and Sci.*, vol.1, no.5: 17-25, 2012.
7. L. Ravisankar, V. Ravichandran, V. Chinnathambi and S. Rajasekar, Effect of Narrow Band Frequency Modulated Force on Horseshoe Chaos in Duffing-vander Pol Oscillator, *Int. J. of Sci. and Eng. Res.*, vol.4, no.8: 1155-1162, 2013.
8. L. Ravisankar, V. Ravichandran, V. Chinnathambi and S. Rajasekar, Horseshoe Dynamics in Asymmetric Duffing-vander Pol Oscillator Driven by Narrow Band Frequency Modulated Force, Chinese J. of Physics, *Chinese J. of Physics*, vol.52, no.3: 1026-1043, 2014.
9. S. Rajasekar and M. Lakshmanan, Controlling of chaos in BVP oscillator, *Int. J. Bifur. Chaos*, vol.2: 201-204, 1992.
10. S. Rajasekar and M. Lakshmanan, Algorithms for controlling chaotic motion : application for the BVP oscillator, *Physica D*, vol.67: 282-300, 1993.
11. B. Ravindra and A.K. Mallik, Stability analysis of a non-linearly damped Duffing oscillator, *J. Sound. Vib.*, vol.171: 708-716, 1994.

12. B. Ravindra and A.K. Mallik, Role of nonlinear dissipation in soft Duffing oscillators, *Phys. Rev. E.*, vol.49: 4950-4954, 1994.
13. A Sharma, V. Patidar, G. Purokit and K.K. Sud, Effects on the bifurcation and chaos in forced Duffing oscillator due to nonlinear damping, *Communications in Nonlinear Science and Numerical Simulation*, vol.176: 2254-2269, 2012.
14. M.S. Soliman and J.M.T. Thompson, The effect of damping on the steady state and basin bifurcation patterns of a nonlinear mechanical oscillator, *Int. J. Bifur. and Chaos*, vol.2: 81-91, 1992.
15. J.P. Baltanas, J.L. Trueba and M.A.F. Sanjuan, Energy dissipation in a nonlinearly damped Duffing oscillators, *Physica D*, vol.159: 22-34, 2001.
16. J. Padovan and J.T. Sawicki, Nonlinear vibration of fractional damped systems, *Nonlinear Dynamics*, vol.16: 321-336, 1198.
17. R.E. Mickons, Fractional Vander Pol equations, *J. Sound. Vib.*, vol.259: 457-460, 2003.
18. R.E. Mickens, K.O. Oyedeji and S.A. Rucker, Analysis of the simple harmonic oscillator with fractional damping, *J. Sound Vib.*, vol.268: 839-842, 2003.
19. Z.M. Ge and C.Y. Ou, Anticontrol of chaos of two degrees of freedom loud speaker system and synchronization of different order systems, *Chaos, Solitons and Fractals*, vol.20: 503-521, 2004.
20. M.A.F. Sanjuan,The effect of nonlinear damping on the universal escape oscillator, *Int. J. Bifur. and Chaos*, vol.9: 735-744, 1999.
21. J. Awerjeewicz and M.M. Holicke, Melnikov method and stick-slip chaotic oscillations in very weakly forced mechanical systems, *Int. J. Bifurcation and Chaos*, vol.9: 505-518, 1999.
22. M. Bikdesh, B. Balachandran and A. Nayfeh, Melnikov's method for a ship with general rool-damping model, *Nonlinear Dynamics*, vol.6: 101-124, 1994.
23. J.L. Trueba, J. Rams and M.A.F Sanjuan, Analytical Estimates of the Eeffect of Nonlinear Damping in some Nonlinear Oscillators, *Int. J. Bifur. and Chaos*, vol.109, 2257-2267, 2000.
24. M. Borowice, G. Litak and A. Syta, Vibration of the Duffing Oscillator; Effect of Fractional Damping, *Shock and Vibration*, vol.14: 29-36, 2007.
25. L.J. Sheu, H.K. Chen, J.H. Chen and L.M. Tam, Chaotic dynamics of the fractionally damped Duffing equation, *Chaos, Solitons, Fractals*, vol.31: 1203-1212, 2007.
26. P.J. Holmes, nonlinear oscillator with a strange attractor, *Phil. Trans. R. Soc. Lond. A*, vol.292: 419-448, 1979.
27. R. Chacon, *Control of Homoclinic Chaos by Weak Periodic Perturbations*, World Scientific, Singapore, 2005.
28. S. Wiggins, Global Bifurcations and Chaos, Springer-Verlag, New York, 1988.
29. E. Simu, *Chaos, Transitions in Deterministic and Stochastic Dynamical Systems*, Princeton Univ. Press, New Jersey, 2002.
30. G. Chen and X. Dong, *From Chaos to Order: Methodologies, Perspectives and Applications*, World Scientific, Singapore, 1998.
31. M. Lakshmanan and S. Rajasekar, *Nonlinear Dynamics, Integrability, Chaos and Patterns*, Springer-Verlag, Berlin, 2003.
32. M. Lakshmanan and K. Murali, *Chaos in Nonlinear Oscillators: Controlling and Synchronization*, World Scientific, Singapore, 1998.
33. M.V. Sethu Meenakshi, S. Athisayanathan, V. Chinnathambi, S. Rajasekar, estimates of the effect of amplitude modulated signal in nonlinearly damped Duffing-vander Pol oscillator, *Chinese Journal of Physics*, vol.55: 2208-2217, 2017.

34. M.V. Sethu Meenakshi, S. Athisayanathan, V. Chinnathambi, S. Rajasekar, Effect of Narrow Band Frequency Modulated Signal on Horseshoe Chaos in Nonlinearly Damped Duffing-vander Pol Oscillator, *Annual Review of Chaos Theory, Bifurcations and Dynamical Systems*, vol.7: 41-55, 2017.
35. H. Simo and P. Woafo, Effects of asymmetric potentials on bursting oscillations in Duffing oscillator, *Optik-Int.J. of Light and Electron Optic*, vol. 127, no.20: 8760-8766, 2016.
36. V. Ravichandran, S. Jeyakumari, V, Chinnathambi S. Rajaseakr and M.A.F. Sanjuan, Role of asymmetries in the chaotic dynamics of the double-well Duffing oscillator, *Pramana J. Phys.*, vol.72, no,6: 927-937, 2009.
37. S. Arathi, S. Rajasekar and J. Kurths, Characteristics of Stochastic Resonance in Asymmetric Duffing oscillator, *Int. J. of Bifur. and Chaos*, vol.21: 2729-2739, 2011.